Fine Precipitates in Nickel Base Superalloys

Ercan Balikci[1,*] and Arun Altincekic[1]

[1]*Department of Mechanical Engineering, Bogazici University, Istanbul, Turkey*

Abstract: Presence of fine, secondary/tertiary precipitates in superalloys improves especially the creep-fatigue properties of these alloys. It is conveniently accepted that the fine precipitates form non-isothermally, for example, during cooling from an aging temperature or isothermally during a secondary, lower temperature aging. In the current study, several single-aging treatments were conducted to assess the formation of the fine precipitates in the polycrystalline, nickel-base superalloy IN738LC. The agings were carried out stress-free at 950°C, 1050°C, 1120°C, and 1140°C for various times. Stressed agings at 950°C and 1050°C were also conducted. A time-dependent isothermal formation of the fine precipitates was observed. The formation time decreased as the aging temperature increased. It is suggested that dissolution of some coarse precipitates, evolution of the precipitate-matrix interface toward a fully faceted one, and increased matrix channel width saturate the channels and control the formation of the fine precipitates.

Keywords: Nibase superalloys, Aging, Precipitation, Faceting, Growth kinetics.

1. INTRODUCTION

The precipitates in superalloys are the major ingredients of strengthening. In nickel-base superalloys, the precipitate phase is the ordered Ni_3Al gamma prime (γ') phase residing in a disordered, solid solution gamma (γ) matrix [1]. The precipitate size distribution, morphology, and volume fraction are crucial for sustaining many mechanical properties of parts produced from superalloys. The precipitate size distribution may be unimodal or multimodal (bimodal, trimodal, etc). While a unimodal size distribution is represented by a single Gaussian, a multimodal size distribution is characterized by more than one Gaussian. The size distribution is pertinent to tensile, creep, fatigue, and specifically creep-fatigue properties. The fine precipitates in a bimodal distribution are believed to strongly interact with the deformation dislocations and eventually affect the creep-fatigue interactions [2]. Therefore, it is of a crucial importance to understand the formation mechanisms of the fine precipitates.

Significant variations observed in the size of precipitates in multimodal microstructures point to multiple nucleation events at well separated times. Following a super-solvus solution treatment, the primary precipitates nucleate and grow during the primary aging stage and are the large ones in a multimodal microstructure, while the medium and small ones form either during a secondary aging at a lower temperature or during cooling from the aging temperature. Hence, the precipitates forming during cooling are called the ''cooling precipitates''. Although multimodal precipitate size distribution is usually observed after slow cooling, [3-7] a multimodal distribution at intermediate [8] and fast [7] cooling rates has also been reported. All these studies have related the formation of a multimodal precipitation to an increased diffusion path of the precipitate forming solute elements; as the primary precipitates grow, the space between them increases, which extends the diffusion distance. Hence, the matrix channels between the precipitates become supersaturated again during cooling, resulting in secondary/tertiary nucleation, which forms the small precipitates.

Furthermore, alloy composition has been found to be a determining factor in the secondary/tertiary nucleation. Mitchell and Preuss [5] have investigated the superalloys Udimet720 and RR1000. They have observed a different behavior in the bimodal precipitation which has been reasoned to the presence of tantalum (Ta) in RR1000. As Ta diffuses slower than Al, precipitation of small particles shortens the diffusion path.

The multimodal precipitation may also occur during an isothermal aging [9]. It has been previously reported [10-12] that the γ' precipitates in the superalloy IN738LC grow isothermally in a unimodal cuboidal morphology up to a critical size, beyond which a bimodal size distribution sets in, where visibly large and small size precipitates coexist. These observations have been attributed to the dissolution of the large precipitates. A concurrent occurrence of partial dissolution of the large precipitates and appearance of the small ones in Udimet720 has been reported [5]. In addition, a bimodal carbide precipitation during an isothermal heating has been associated with the co-

*Address correspondence to this author at the Department of Mechanical Engineering, Bogazici University, Istanbul, Turkey; Tel: +90-212-3597353; E-mail: ercan.balikci@boun.edu.tr

E-ISSN: 2410-4701/19

existence of partitional and partitionless growth [13]. Another evidence for the isothermal formation of fine precipitates has been reported by Sisi Xiang *et al.* [14]. Although the suggested fine precipitates formed at nodes of interfacial dislocation networks are dubious as pointed out by Cormier *et al*. [15], ones forming away from the interface are plausible. Assuming that all experiments have been conducted (heated to and kept at the test temperature and cooled) in a similar manner, observation of fine precipitates in longer creep times suggest that the only parameter leading to precipitation of secondary, fine precipitates is the variation in time. Reported growth of the fine precipitates also suggest that they form and evolve during isothermal creep tests [14].

The γ' precipitates in nickel-base superalloys grow coherently with their matrix. Any difference in the lattice parameters of the precipitates and matrix leads to a misfit at the interface. Therefore, growing coherent precipitates may put the interface under a compressive or tensile stress. When the lattice parameter of the precipitate is larger than that of the matrix, the interface on the precipitate side is under compression. Consequently, the strained interface influences the diffusion of the solute elements into the precipitates. Furthermore, as the precipitates grow, they develop flat, faceted faces aligned with the weak elastic directions of the <001> type. The ordered nature of the flat, planar faces should possess a lower accommodation factor for diffusional jumps compared to a curved, rough interface that exists during the early stages of the growth [16].

This study assesses the isothermal, time-dependent formation of the fine, secondary precipitates during isothermal stress-free agings and isothermal stressed (compressive and tensile) agings. Experimental observations are presented to suggest a mechanism for the fine precipitate formation. As the fine precipitates in a multimodal precipitate microstructure has a crucial role in the high temperature creep, fatigue, and creep-fatigue behavior of superalloys, this current manuscript will shed a light on the understanding of the formation mechanisms of the fine precipitates.

2. EXPERIMENTAL

The material used was a polycrystalline Ni-base cast superalloy IN738LC. In its as-received condition, it was HIPed (hot isostatically pressed) and was given a standard aging treatment by the manufacturer [10]. The microstructure of this as-received stock already contained multimodal distribution of the precipitates and so was not suitable to study formation mechanism of a bimodal size distribution. Hence, stress-free and stressed (compressive and tensile) aging heat treatments followed a solution treatment at 1200^{o}C for 4 hours and water quenching. 4-mm thick quarter disks were cut from 15-mm diameter bars for stress-free aging heat treatments. Stressed agings under compressive stress were conducted with conical specimens where the stress varied from 56 to 224 MPa at 950^{o}C and from 28 to 112 MPa at 1050^{o}C. Tensile stress agings were carried out with a standard creep specimen of 6 mm reduced section diameter and 56 to 112 MPa stress. Table **1** gives the heat treatment schedules. During the stress-free agings the samples were in a vacuumed quartz tube, and in stressed agings they were in a protective argon environment. The stress-free samples were water quenched directly after aging by tilting the furnace whereas the stressed samples were cooled in the furnace by powering off and opening the covers of the furnace to achieve the rate of air cooling. The average furnace cooling rate was measured as 12.0 ^{o}C/minute until the temperature fell to 600^{o}C, below which the precipitation kinetics was very low [10]. A tubular furnace was used in all of the experiments.

Subsequent to the heat treatments, the samples were prepared for microscopic analysis by metallographic grinding and polishing. They were then etched with a solution containing, by volume, 33 pct. HNO_3, 33 pct. CH_3COOH, 33 pct. H_2O, and 1 pct. HF. A PHILIPS XL30E SEM-FEG/EDAX system with 2 nm spatial resolution was used to observe the γ' precipitates. A backscattered electron detector was used in the scanning electron microscope (SEM) because of its higher composition sensitivity. This yields a good contrast in the SEM images where the matrix appears as a light background and the precipitates show up as dark particles. The microphotographs were taken at several magnifications up to 120,000X and with accelerating voltages from 10 to 25 kV to resolve the extremely fine precipitates. The precipitate sizes were then measured from the digital micrographs using the ImageJ image processing software [17]. The precipitate size data was obtained using 15kX and 30kX photos for the coarse ones and 120kX photos for fine precipitates. The size data was used to calculate the area fraction of the precipitates and the width of the matrix channel between the primary precipitates. The channel width for some

Table 1: Heat Treatment Schedules

Solution Treatment	Aging Treatments
1200°C / 4h /WQ	950°C/t/WQ t = 0.5, 2, 12, 24. t = 24, 192, 480, 960 with σ_c = 56 – 224 MPa
	1050°C/t/WQ t = 24, 48, 96, 144, 192, **288, 480.** t = 24, **192, 480** with σ_c = 28 – 112 MPa. t = 1.5, 3, 22, 30, **164** with σ_T = 85, 112, 85, 85, 56 MPa respectively.
	1120°C/t/WQ t = 0.25, **0.5, 2, 12, 24**.
	1140°C/t/WQ t = 0.0166, 0.083, **0.166, 0.25, 0.33, 0.5.**
WQ = water quenched; t = time (hour); $\boldsymbol{\sigma_c}$ = compressive stress; $\boldsymbol{\sigma_T}$ = tensile stress. Agings with stress are concluded with a cooling rate of 12°C/minute. **Bold numbers** show the time of fine precipitate formation.	

samples was measured as well. The samples were all from the same alloy batch and the same procedures at all stages of the experimentations and analyses were adopted.

3. RESULTS AND DISCUSSION

After various isothermal single-aging treatments (Table **1**), a bimodal precipitate size distribution is observed in certain samples as seen in Figure **1e** where the large dark particles (partially seen in the photo due to magnification) are the primary precipitates and the fine dark particles are the secondary precipitates. The latter ones are first attributed to the cooling precipitates, as they are already accepted and documented in the literature [6]. Nevertheless, as the aging time has been varied isothermally, a time-dependent bimodal precipitate size distribution is noticed. As seen in Figure **1**, the fine precipitates do not appear until 288 hours of aging at 1050°C. A similar bimodal precipitate size distribution appears just after 30 minutes at 1120°C and after 10 minutes at 1140°C. Yet, a unimodal size distribution is preserved in the single-agings at 950°C up to 24 hours and possibly way beyond 288 hours, not used at this temperature in this study. Conversely, fine precipitates are observed after 192-hour and 480-hour agings at 1050°C and not earlier than 24 hours when samples are aged under compressive stress. Of course, they may form at a time between 24 and 192 hours. Samples aged under tensile stress show fine precipitates after 164 hours at 1050°C and could possibly occur somewhat earlier too. Obviously, since the amount of the super-saturation is fixed and a multiple nucleation event is not normally expected at a given temperature, these observations seem to contradict the convention.

The formation of a bimodal precipitate microstructure is generally attributed to a matrix saturation during cooling. The matrix supersaturation for a given composition in an alloy system is determined by its phase diagram and is fixed for a given temperature, but increases with decreasing the temperature. This saturation governs the precipitation reaction at the temperature. Thus, during an isothermal aging, precipitate forming solute atoms diffuse in the matrix to nucleate, grow, and then coarsen a precipitate [18-22]. As the primary precipitates grow isothermally the precipitate spacing and so the diffusion path for the precipitate forming solute atoms increases. Thus, a nucleation event can take place in the matrix channels between the well- spaced primary precipitates during cooling, depending on the counteracting rates of the matrix depletion via the coarsening and the matrix saturation needed for a new nucleation event [6, 7, 23]. Therefore, multiple nucleation events may take place during cooling, yielding a multimodal precipitate microstructure containing the fine ‘‘cooling precipitates’’.

Alternatively, the fine precipitates might already form during an aging [9] as a result of an isothermal saturation of the matrix channels between the primary precipitates. This may happen because of a mode change from a diffusional to interface and/or mixed

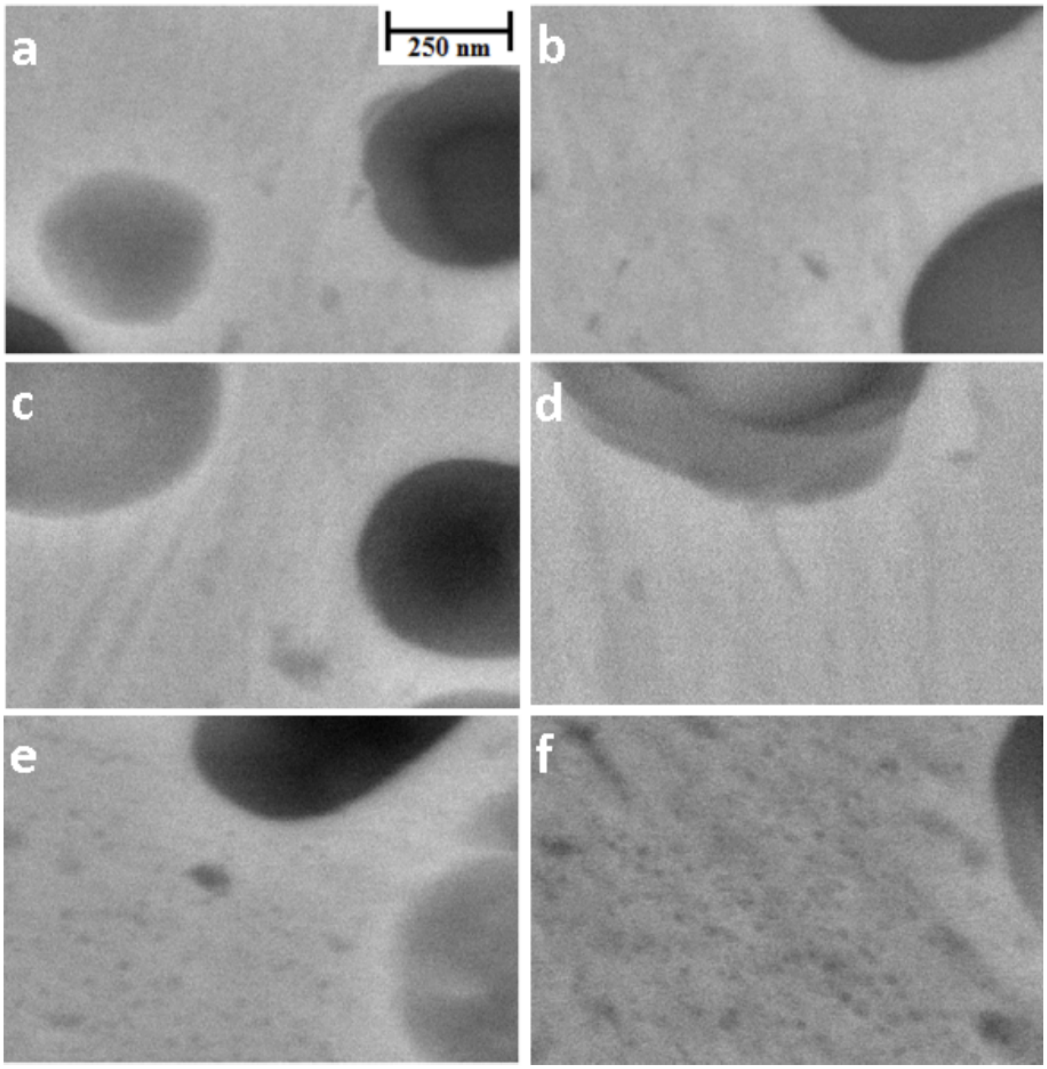

Figure 1: Micrographs of specimens aged stress-free at 1050 ^{o}C for **a**) 48, **b**) 96, **c**) 144, **d**) 192, **e**) 288, **f**) 480 hours. Dark particles are the precipitates and gray background is the matrix. Note the fine precipitates only in e and f. The large precipitates are partially seen due to magnification of 60kX.

controlled growth for the primary precipitates and an increase in the matrix channel width. This suggestion relies on two factors. First, there should be enough solute atoms in the matrix. Second, a barrier should develop in transient to decelerate joining of these solute atoms to the already existing primary precipitates, so the matrix can supersaturate in time. Actually, in addition to the solute already present in the matrix, dissolution of the primary precipitates may be a source for the new solute. It has been reported that the growth of large, coherent precipitates becomes extremely slow [24] and cannot be sustained beyond a critical size due to vastly increased misfit strain energy [10, 25], so the precipitate dissolution may set in [5, 8, 11, 26-29]. The dissolution has been observed along the precipitate corners [11, 27]. In fact, the precipitate coarsening and dissolution are simultaneous processes [5, 8]. Actually, a prolonged aging has been found to oversaturate the matrix with elements like W, Ta, and Al [30]. Hence, these isothermal events can supply the matrix with precipitate forming solute atoms. Then, the barrier is generated by the evolution of the precipitate-matrix interface toward a fully faceted one and the increased diffusion path by the widening matrix channels.

The growth of second phase particles in a matrix can be due to a diffusion-controlled or an interface-controlled mechanism [18]. The time dependency of the precipitate size distribution in the nickel base superalloys is mostly treated according to the Lifshitz and Slyozov [19] and Wagner theory [20], which relies on the solute diffusion in the matrix and underestimate the role of the precipitate-matrix interface which was

already pointed out in the 1970s [16]. Recently, the interface-limited species transport has been revisited by Ardell and Ozolins, considering the interface properties, and a trans-interface diffusion-controlled coarsening (TIDC) model has been proposed [31]. In their suggestion, the interface is a partially ordered diffuse one, bounded by an ordered precipitate and a disordered matrix [32]. Hence, the partially ordered diffuse interface is a diffusion bottleneck. The width of this structurally diffuse region depends on the precipitate size [31] and, as documented by atom probe tomography (APT), the rate of cooling after aging [33] and the isothermal aging time [34, 35]. A temperature and composition dependency of the interface width has been reported recently [36]. A diffuse interface has also been simulated by a phase field model [37].

The role of the interface can be appreciated by recalling that the cuboidal γ' precipitates have $L1_2$ ordered crystal structure with flat faces (facets) which should show a lateral ledge growth mode [36]. Thus, a lateral ledge growth in the ordered flat interfaces can operate with a lower accommodation factor in comparison with the continuous growth that operates in a disordered structure [16, 18]. Nevertheless, the ledge growth kinetics should be effective after formation of well-developed cube faces (facets) [38].

In addition, a positive misfit, in the case of the superalloy IN738LC, [25] puts the interface on the precipitate side under a compressive stress, which may increase in magnitude with precipitate size and may not accommodate the incoming solute atoms [39]. Moreover, an interface dislocation network (a cage) may develop during aging especially in the presence of an external load [40], so it prevents precipitate coarsening [12, 41, 42] because it acts as a barrier for solute transfer through the interface, unlike being a pipe diffusion path [43, 44]. Hence, an ordered, strained, and caged interface may prevent the solute diffusion to the precipitates for their growth, which keeps the solute atoms in the matrix.

In fact, a solute build up at a partially ordered interface has been simulated in the TIDC model [31]. Furthermore, a more diffuseness towards the matrix side detected by the APT [35] indicates a solute build up in the near interface matrix region because of a slower diffusivity in the ordered precipitate. This indicates that the precipitate formers can now saturate the matrix to form the fine, secondary precipitates within the matrix channels via the classical nucleation and growth mechanism [18].

In addition, our observations suggest that time dependent, isothermal precipitation of the fine precipitates requires a critical primary precipitate spacing, the matrix channel width, as also reported by others [8, 15, 45]. After a phase field modeling, Boussinot *et al*. have observed an isothermal bimodal precipitation in the wide channels [2]. However, when the channel width is small, the large precipitates interact and do not allow the formation of the fine precipitates. This modeling result suggests that formation of the bimodal precipitate microstructure is more plausible when the volume fraction of the large precipitates is low, which results in a wide matrix channel. Nevertheless, a very low volume fraction of the precipitates implies a low solute content that may not be enough to re-saturate the very wide matrix channels. In fact, the precipitate volume fraction in the positive misfit, polycrystalline superalloy IN738LC (~ 40%) is midway between those in the dilute alloys (~ 5 – 20%) and those in the negative misfit single crystal superalloys (~ 70%).

The channel width is calculated from the measured precipitate area fraction data for stress-free agings at 1050^{o}C as given in Figure **2**. Although a single data point at 144 hours do not fall in the trend, the closeness of the measured and calculated matrix channel widths validates the correctness of the image analysis procedure. As we have checked carefully the outlier data point at 144 hours, the reason for this behavior is unknown. The area fraction of the large precipitates decreases when the fine ones form, similar to that reported by Mitchel and Preuss [5]. The channel width increases linearly with the aging time after 192 hours. As a result, the secondary precipitates are observed in isothermal agings after 288 hours at 1050^{o}C. The time required for a bimodal precipitation decreases with an increase in the aging temperature. For example, it is 10 minutes at 1140^{o}C and 30 minutes at 1120^{o}C. Nevertheless, when the superalloy is aged at 950^{o}C, no secondary fine precipitate is seen after stressed-agings up to 960 hours. This indicates that in the latter case, the solute remaining in the matrix cannot precipitate out as fine ones either during aging or during cooling. That is because the growing precipitates are not large enough to develop a fully faceted interface acting as a diffusion barrier as outlined in the earlier paragraphs above. Moreover, the width is not large enough for saturation and the diffusion rate is considerably lower at this temperature.

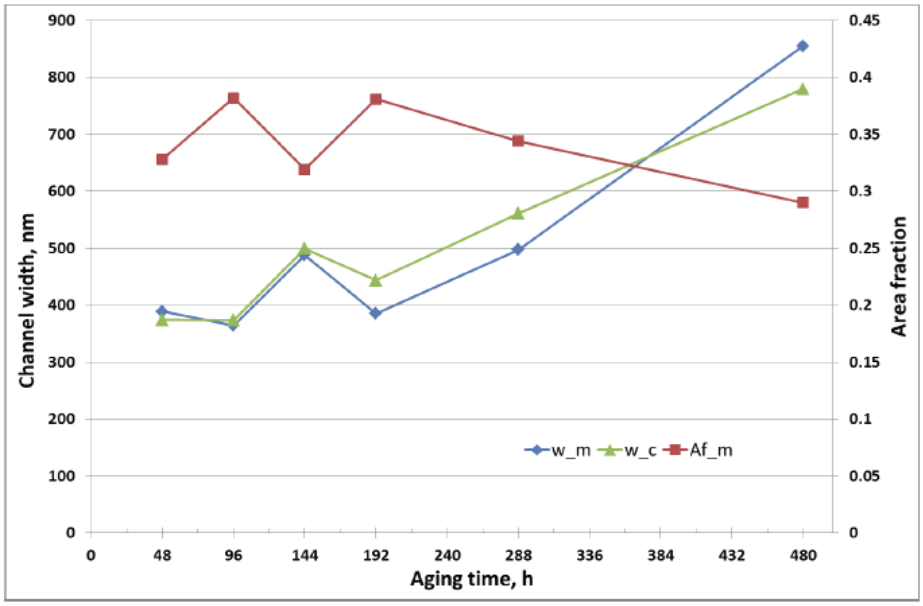

Figure 2: The measured (w,m) and calculated (w,c) matrix channel width and the measured area fraction (Af,m) of the coarse precipitates in samples aged stress-free at 1050°C.

Furthermore, interacting strain and composition fields can alter the growth behavior of the precipitates [46-48]. In fact, at 1050°C, the bimodal size distribution is detected after 288 hours in stress-free aged samples whereas this distribution at the same temperature is observed after a shorter (192 hours) time in compressive stress-aged samples at 28, 56, and 112 MPa stress levels. In the tensile aged specimens, fine precipitates are observed in a sample aged for 164 hours at 56 MPa stress. It is expected that the applied stress should modify the precipitate – matrix interface stress distribution differently depending on the level and sign of the applied stress. This then influences fine precipitate formation kinetics, since stress can modify the magnitude of diffusion in the matrix, through the interface, and in the precipitate. Of course, a thorough analysis of stress distribution in the matrix channels and at the interface is necessary to elaborate more unequivocally on the effect of stress on the formation of fine precipitates.

In addition, the fine precipitates show a size dependence on the time and stress [12]. If these precipitates form only during cooling, they should form after all the isothermal aging treatments irrespective of the aging time and they all should have similar size because they cool from the same temperature with the same cooling rate. Hence, they all should be visible / invisible in the scanning electron microscope (SEM) observations.

The precipitate microstructures have been analyzed by the SEM in the back scattered electron (BSE) mode with magnifications up to 120,000X. In addition to this high magnification, accelerating voltages of 10, 15, 20, and 25 kV have been used in the SEM to assess and improve visibility of the secondary, fine precipitates. It has been found that 10 kV is the most appropriate voltage to distinguish the fine precipitates as seen in Figure **3**. Usually, a high accelerating voltage is preferred to excite more electrons to help the visibility, although an excessive excitation can cause loss of sharpness especially at the corners and edges due to the charging. In fact, it has been shown that use of low accelerating voltages in the BSE mode can increase the resolution in the near surface region by reducing the spread in the BSE signal and the beam interaction volume in the sample [50-52]. In the present case, the incoming electron beam excites both the matrix and the fine precipitates, and a signal overlap may be occurring at the higher voltages. The fine precipitates may contain more of those elements (*e.g.*, Cr, Co, and Mo) that normally segregate to the matrix in later stages of their growth [30]. Conversely, segregation of the precipitate forming elements (*e.g.*, Al and Ti) to the fine precipitates is incomplete [53]. Thus, when the matrix and the fine precipitates are excited together with the higher voltages (larger beam interaction volume), the fine precipitates go invisible because the excitation from them is lost within that of the matrix due to a lower concentration contrast.

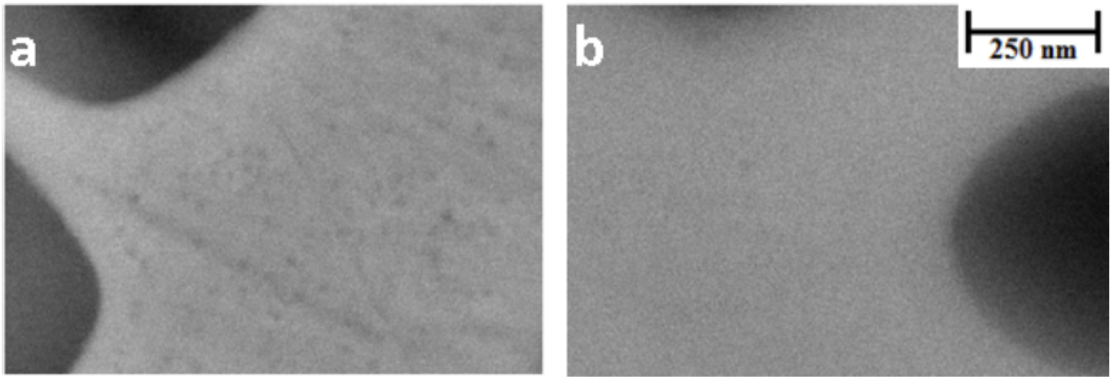

Figure 3: Micrographs of a specimen aged stress-free at 1050°C for 288 hours. The SEM images are taken at 60kX magnification with accelerating voltages of **a**) 10 kV and **b**) 20 kV. The fine precipitates are seen only in **a**).

CONCLUSIONS

It is proposed that fine precipitates can occur isothermally within the matrix channels between the primary coarse precipitates. This suggestion relies on two factors, a faceted interface with low accommodation for the precipitate forming solute atoms and an optimally wide matrix channel width. The gamma prime precipitates possess an ordered crystal structure, so their growth should be governed by ledges on the cube faces and the growth should take place laterally. This may lower solute attachment to the precipitates and keep the solute in the matrix channels. Furthermore, an optimally wide matrix channel width prevents interaction between the primary precipitates. Thus, saturation in the matrix channels can increase leading to nucleation and formation of the fine precipitates isothermally.

REFERENCES

[1] RC. Reed: The Superalloys-Fundamentals and Applications, 1st ed., Cambridge University Press, New York, NY, 2006; pp. 40-49.

[2] G. Boussinot, A. Finel, and Y. Le Bouar: Acta Mater 2009; 57; 921-931. https://doi.org/10.1016/j.actamat.2008.10.039

[3] S. Behrouzghaemi and RJ. Mitchell: Mater Sci Eng A 2008; 498: 266-271. https://doi.org/10.1016/j.msea.2008.07.069

[4] RJ. Mitchell, M. Preuss, MC. Hardy, and S. Tin: Mater Sci Eng A 2006; 423: 282-291. https://doi.org/10.1016/j.msea.2006.02.039

[5] RJ. Mitchell and M. Preuss: Metall Mater Trans A 2007; 38A: 615-627. https://doi.org/10.1007/s11661-007-9089-6

[6] J. Mao, K. Chang, W. Yang, K. Ray, SP. Vaze, and DU. Furrer: Metall Mater Trans A 2001; 32A: 2441-2452. https://doi.org/10.1007/s11661-001-0034-9

[7] PM. Sarosi, B. Wang, JP. Simmons, Y. Wang, and MJ. Mills: Scripta Mater 2007; 57: 767-770. https://doi.org/10.1016/j.scriptamat.2007.06.014

[8] YH. Wen, JP. Simmons, C. Shen, C. Woodward, and Y. Wang: Acta Mater 2003; 51: 1123-1132. https://doi.org/10.1016/S1359-6454(02)00516-5

[9] E. Balikci and D. Erdeniz: Metall Mater Trans A 2010; 41A: pp. 1391-1198. https://doi.org/10.1007/s11661-010-0241-3

[10] E. Balikci, A. Raman, and RA. Mirshams: Metall Mater Trans A 1997; 28A: 1993-2003. https://doi.org/10.1007/s11661-997-0156-9

[11] E. Balikci, RA. Mirshams, and A. Raman: Z Metallkd 1999; 90(2): 132-140.

[12] A. Altincekic and E. Balikci: Metall Mater Trans A 2013; 44A: 2487-2498. https://doi.org/10.1007/s11661-013-1618-x

[13] Q. Chen, K. Wu, G.Sterner, and P.Mason: J Mater Eng Perform 2014; 23: 4193-4196. https://doi.org/10.1007/s11665-014-1255-6

[14] S. Xiang, S. Mao, H. Wei, Y. Liu, J. Zhang, Z. Shen, H. Long, H. Zhang, X. Wang, Z. Zhang, and X. Han: Acta Mater 2016; 116: 343-353. https://doi.org/10.1016/j.actamat.2016.06.055

[15] J. Cormier, V. Caccuri, JB. Graverend, P. Villechaise: Scripta Mater 2017; 129: 100-103. https://doi.org/10.1016/j.scriptamat.2016.10.012

[16] HI. Aaranson: J. Microsc 1974; 102: 275-300. https://doi.org/10.1111/j.1365-2818.1974.tb04640.x

[17] WS. Rasband: Image J, US. National Institutes of Health, Bethesda, MD, 1997-2007. http://rsb.info.nih.gov/ij/.

[18] RD. Doherty: Met Sci 1982; 16: 1-13. https://doi.org/10.1080/0031322X.1982.9969649

[19] IM. Lifshitz and VV. Sloyozov: J Phys Chem Solids 1961; 19(1-2): 35-50. https://doi.org/10.1016/0022-3697(61)90054-3

[20] C. Wagner: Z. Elektrochemie 1961; 65(7-8): 581-591. https://doi.org/10.1001/archopht.1961.01840020583023

[21] AJ. Ardell: Acta Metall 1972; 20(1): 61-71. https://doi.org/10.1016/0001-6160(72)90114-9

[22] AD. Brailsford and P. Wynblatt: Acta Metall 1979; 27(3): 489-497. https://doi.org/10.1016/0001-6160(79)90041-5

[23] C. Ahn, N. Bennett, ST. Dunham, and NEB. Cowern: Phys Rev B 2009; 79(7): 073201-1-073201-4. https://doi.org/10.1103/PhysRevB.79.073201

[24] RS. Moshtaghin and S. Asgari: Mater. Des 2003; 24: 325-330. https://doi.org/10.1016/S0261-3069(03)00061-X

[25] E. Balikci, R.E. Ferrell, Jr., and A. Raman: Z. Metallkd 1999; 90: 141-146.

[26] G. Wang, DS. Xu, N. Ma, N. Zhou, EJ. Payton, R. Yang, MJ. Mills, and Y. Wang: Acta Mater 2009; 57: 316-325. https://doi.org/10.1016/j.actamat.2008.09.010

[27] AB. Parsa, P. Wollgramm, H. Buck, A. Kostka, C. Somsen, A. Dlouhy, and G. Eggeler: Acta Mater 2015; 90: 105-117. https://doi.org/10.1016/j.actamat.2015.02.005

[28] A.K. Dwarapureddy, E. Balikci, S. Ibekwe, and A. Raman: J Mater Sci 2008; 43: 1802-1810 https://doi.org/10.1007/s10853-007-2342-y

[29] I. Roy, E. Balikci, S. Ibekwe, and A. Raman: J Mater Sci 2005; 40: 6207-6215. https://doi.org/10.1007/s10853-005-3154-6

[30] R. Schmidt and M. Feller-Kniepmeier: Metall Trans A 1992; 23A: 745-757. https://doi.org/10.1007/BF02675552

[31] AJ. Ardell and V. Ozolins: Nat. Mater 2005; 4: 309-316. https://doi.org/10.1038/nmat1340

[32] S. Meher, T. Rojhirunsakool, P. Nandwana, J. Tiley, and R. Banerjee: Ultramicroscopy 2015; 159: 272-277. https://doi.org/10.1016/j.ultramic.2015.04.015

[33] XP. Tan, D. Mangelinck, C. Perrin-Pellegrino, L. Rougier, Ch.-A. Gandin, A. Jacot, D. Ponsen, and V. Jaquet: Metall. Mater. Trans. A, 2014; 45A: 4725-4730. https://doi.org/10.1007/s11661-014-2506-8

[34] XP. Tan, D. Mangelinck, C. Perrin-Pellegrino, L. Rougier, Ch.-A. Gandin, A. Jacot, D. Ponsen, and V. Jaquet: J. Alloy Compd 2014; 611: 389-394. https://doi.org/10.1016/j.jallcom.2014.05.132

[35] JY. Hwang, S. Nag, ARP. Singh, R. Srinivasan, J. Tiley, HL. Fraser, and R. Banerjee: Scripta Mater 2009; 61: 92-95. https://doi.org/10.1016/j.scriptamat.2009.03.011

[36] F. Forghani, JC. Han, J. Moon, R. Abbaschian, CG. Park, HS. Kim, and M. Nili-Ahmadabadi: J. Alloy Compd 2019; 777: 1222-1233. https://doi.org/10.1016/j.jallcom.2018.10.128

[37] LT. Mushongera, M. Fleck, J. Kundin, Y. Wang, and H. Emmerich: Acta Mater 2015; 93: 60-72. https://doi.org/10.1016/j.actamat.2015.03.048

[38] GC. Weatherly: Acta Metall 1971; 19: 181-192. https://doi.org/10.1016/0001-6160(71)90145-3

[39] PK. Footner and B.P. Richards: J Mater Sci 1982; 17: 2141-2153. https://doi.org/10.1007/BF00540433

[40] A. Altincekic and E. Balikci: Metall. Mater Trans A 2014; 45A: 5923-5936. https://doi.org/10.1007/s11661-014-2558-9

[41] R. Schmidt and M. Feller-Kniepmeier: Scripta Metall. Mater 1993; 29: 1079-1084. https://doi.org/10.1016/0956-716X(93)90181-Q

[42] A. Epishin, T. Link, and G. Nolze: J Microsc 2007; 228: 110-117. https://doi.org/10.1111/j.1365-2818.2007.01831.x

[43] RD. Vengrenovich, YV. Gudyma, and S.V. Yarema: Phys Met Metallogr 2001; 91(3): 228-232.

YM. Ustyugov: Phys Met Metallogr 2007; 104: 453-460. https://doi.org/10.1134/S0031918X07110038

[44] JB. Le Graverend, J. Cormier, F. Gallerneau, and P. Paulmier: Adv Mat Res 2011; 278: 31-36. https://doi.org/10.4028/www.scientific.net/AMR.278.31

[45] RA. Ricks, AJ. Porter, and RC. Ecob: Acta Metall 1983; 31(1): 43-53. https://doi.org/10.1016/0001-6160(83)90062-7

[46] M. Doi, T. Miyazaki, and T. Wakatsuki: Mater Sci Eng 1984; 67(2): 247-253. https://doi.org/10.1016/0025-5416(84)90056-9

[47] PW. Voorhees and WC. Johnson: J Chem Phys 1986; 84(9): 5108-5121. https://doi.org/10.1063/1.450664

[48] WC. Johnson and PW. Voorhees: J Appl Phys 1987; 61: 1610-1619. https://doi.org/10.1063/1.338099

[49] RG. Richards, G.Rh. Owen, and I. ap Gwynn: Scanning Microscopy 1999; 13(1): 55-60.

[50] KL. Lee, M. Ward: J Vac Sci Technol B 1991; 9(6): 3590-3596. https://doi.org/10.1116/1.585851

[51] Radis R. Radis, M. Schaffer, M. Albu, G. Kothleitner, P. Pölt, and E. Kozeschnik: Acta Metall Mater 2009; 57(19): 5739-5747. https://doi.org/10.1016/j.actamat.2009.08.002

[52] J. Li and RP. Wahi: Acta Metall Mater 1995; 43(2): 507-517. https://doi.org/10.1016/0956-7151(94)00252-D

Received on 24-6-2019 Accepted on 15-7-2019 Published on 29-7-2019

DOI: https://doi.org/10.31875/2410-4701.2019.06.1